Int. J. Solids Structures Vol. 29, No. 11, pp. 1433–1451, 1992
Printed in Great Britain.

0020-7683/92 $5.00 + .00

ADVANCED DEVELOPMENT OF BOUNDARY ELEMENT METHOD FOR TWO-DIMENSIONAL DYNAMIC ELASTO-PLASTICITY

A. S. M. ISRAIL and P. K. BANERJEE
Department of Civil Engineering, State University of New York at Buffalo,
240 Ketter Hall, Buffalo, NY 14260, U.S.A.

(*Received* 14 *August* 1990; *in revised form* 6 *September* 1991)

Abstract—In this paper, the formulation and numerical implementation of two-dimensional transient dynamic elasto-plasticity by the boundary element method is presented. This formulation considers material non-linearity and is based on an initial stress approach. It is the first ever attempt to solve two-dimensional dynamic plasticity problems by the boundary element method. The boundary integral equations are cast in an incremental form and are solved using a time stepping technique. The Newton–Raphson iterative scheme is adopted in conjunction with the non-linear constitutive equation to determine the incremental initial stresses. This formulation incorporates quadratic isoparametric elements for both the boundary and volume discretizations. The accuracy and stability of the methodology are demonstrated via numerical examples. It has been implemented in a general purpose, multi-region boundary element software known as GPBEST.

INTRODUCTION

There has been a considerable amount of work done in the area of dynamics by the boundary element method. Most of the research was focused on linear elastodynamic problems using transform domain formulations, i.e. Laplace and Fourier domains. However, linear elastic behavior is at best a first order approximation. Most problems in the real world exhibit non-linear material behavior. Thus the need for a dynamic elasto-plastic algorithm cannot be overemphasized. The transform domain formulations cannot be extended to non-linear problems because of the concept of superposition involved. For this type of problem the algorithm must be based on a time-domain formulation. Mansur (1983) was the first to present a two-dimensional time-domain boundary element formulation using a two-dimensional transient fundamental solution. But his formulation involved very complicated terms. Later, Israil and Banerjee (1990a,b) offered a simplified time-domain formulation using simpler transient kernel functions which produced very accurate solutions. This linear time-domain formulation is a precursor to the non-linear transient dynamic algorithm presented in this paper.

The boundary element method has proven to be a very effective numerical tool for problems involving infinite and semi-infinite domains since the radiation condition is automatically satisfied by the Green function (kernels) used in the formulation. Thus, there is no need to model the far-field. In addition, for linear problems, only the boundary of the domain needs to be discretized. However, for non-linear problems, the part of the volume where non-linearity is expected, needs to be discretized as well. Although the number of unknowns in the resulting algebraic system of equations depends only on the boundary discretization. Still a considerable reduction in computational time and effort is achieved compared to other domain-based methods. In this context, reference can be made to a number of books on the subject, e.g. Banerjee and Butterfield (1981), Mukherjee (1982), etc.

In recent years, quite a number of works have been developed for solving non-linear problems by the boundary element method. Riccardella (1973) presented the two-dimensional and Banerjee *et al.* (1979), the three-dimensional formulations. Cathie and Banerjee (1980) developed the axisymmetric elasto-plastic form. All of these works were focused on static problems. First, a dynamic elasto-plastic BEM formulation was proposed by Ahmad and Banerjee (1990) for three-dimensional problems and they used an iterative algorithm similar to that used by Banerjee and Raveendra (1986). The present work is the

first attempt at two-dimensional problems of dynamic plasticity and it utilizes the Newton Raphson iterative scheme recently proposed by Chopra and Dargush (1991).

BOUNDARY INTEGRAL EQUATION FOR DYNAMIC PLASTICITY

Under zero initial conditions and zero body forces, the boundary integral equation for dynamic plasticity can be written in an incremental form as (Banerjee and Butterfield, 1981; Ahmad and Banerjee, 1990):

$$c_{ij}(\xi)\Delta u_j(\xi,t) = \int_S [G_{ij}(x,t;\xi,\tau) * \Delta t_j - F_{ij}(x,t;\xi,\tau) * \Delta u_j]\,\mathrm{d}S(x) + \int_V B_{ikj}(x,t;\xi,\tau) * \Delta\sigma^0_{ik}\,\mathrm{d}V(x), \quad (1)$$

where

$$B_{ikj} = \frac{1}{2}\left(\frac{\partial G_{ij}}{\partial x_k} + \frac{\partial G_{kj}}{\partial x_i}\right).$$

c_{ij} is the so-called "jump term"; t_i and u_i are traction and displacement vectors, respectively; Δ denotes incremental quantity; $*$ indicates convolution; $\Delta\sigma^0_{ik}$ stands for initial stress; and V indicates the volume of the body.

The terms G_{ij} and F_{ij} are the transient displacement and traction kernels, respectively, and represent the displacements and tractions at a point x at time t due to a unit point force applied at ξ at a preceding time τ. These kernels have been presented in Israil and Banerjee (1990a).

The incremental initial stresses appearing in eqn (1) are derived from the interior stress equation which is given by:

$$\Delta\sigma_{ij}(\xi,t) = \int_S [G^\sigma_{kij}(x,t;\xi,\tau) * \Delta t_k - F^\sigma_{kij}(x,t;\xi,\tau) * \Delta u_k]\,\mathrm{d}S(x) + \int_V P_{kkij}(x,t;\xi,\tau) * \Delta\sigma^0_{kl}\,\mathrm{d}V(x) + J_{kkij}\Delta\sigma^0_{kl}, \quad (2)$$

where G^σ_{kij} and F^σ_{kij} are the transient interior stress kernels and can be found in Israil and Banerjee (1991). The term P_{kkij} is defined as,

$$P_{kkij} = \frac{2\mu\nu}{(1-2\nu)}\delta_{ij}\frac{\partial B_{klm}}{\partial\xi_m} + \mu\left(\frac{\partial B_{kli}}{\partial\xi_j} + \frac{\partial B_{klj}}{\partial\xi_i}\right).$$

In the above expression, δ_{ij} is the Kronecker delta; μ and ν are the shear modulus and Poisson's ratio respectively.

The volume kernel appearing in eqn (2) is strongly singular. Hence, it must be evaluated over $(V - V_\varepsilon)$ as $V_\varepsilon \to 0$ where V_ε is a circular exclusion around ξ. The tensor J_{kkij} is the jump term coming out of the analytical integration of P_{kkij} over V_ε. This jump term is the same as that of the static plasticity and is independent of the size of the exclusion V_ε provided the body has a locally homogeneous initial stress distribution. Its evaluation will be discussed later.

Because of the strong nature of singularity of terms in eqn (2), it cannot be used to obtain the incremental stresses at points on or near the boundary. Thus an alternate procedure is followed to obtain those quantities utilizing boundary solutions. The following set of relations is used in this procedure:

$$\Delta\sigma_{ij}(\xi^b,t)=\left[\frac{2\mu\nu}{(1-2\nu)}\delta_{ij}\Delta u_{k,k}(\xi^b,t)+\mu\{\Delta u_{i,j}(\xi^b,t)+\Delta u_{j,i}(\xi^b,t)\}\right]-\Delta\sigma^0_{ij}(\xi^b,t) \tag{3a}$$

$$\Delta t_i(\xi^b,t)=\Delta\sigma_{ij}(\xi^b,t)n_j(\xi^b) \tag{3b}$$

$$\frac{\partial\Delta u_i}{\partial\eta_z}=\frac{\partial\Delta u_i}{\partial\xi^b_j}\frac{\partial\xi^b_j}{\partial\eta_z}, \tag{3c}$$

where η_z are the set of local axes at the field point (ξ^b).

Equations (3a, b, c) can be solved for the $\Delta\sigma_{ij}$ in terms of incremental tractions, displacements and stresses without the need for temporal or spatial integrations.

VOLUME KERNELS FOR PLASTICITY

The volume kernels B_{ikj} and P_{klij} appearing in eqns (1) and (2) respectively have been derived using the causality of each kind of wave as explained in Israil and Banerjee (1990a). The kernels take the following form:

$$B_{ikj}=\frac{1}{2\pi\rho r}\left\{\frac{1}{c_1}H\left(\frac{c_1t'}{r}-1\right)\left[\frac{1}{\left\{\left(\frac{c_1t'}{r}\right)^2-1\right\}^{3/2}}\left(\frac{C_1}{r}\right)+\frac{2\left(\frac{c_1t'}{r}\right)^2-1}{\sqrt{\left(\frac{c_1t'}{r}\right)^2-1}}\left(\frac{C_2}{r}\right)\right]\right.$$

$$\left.-\frac{1}{c_2}H\left(\frac{c_2t'}{r}-1\right)\left[\frac{1}{\left\{\left(\frac{c_2t'}{r}\right)^2-1\right\}^{3/2}}\left(\frac{C_3}{r}\right)+\frac{2\left(\frac{c_2t'}{r}\right)^2-1}{\sqrt{\left(\frac{c_2t'}{r}\right)^2-1}}\left(\frac{C_2}{r}\right)\right]\right\}$$

and

$$P_{klij}=\frac{\mu}{2\pi\rho r^2}\left\{-\frac{1}{c_1}H\left(\frac{c_1t'}{r}-1\right)\left[\frac{1}{\left\{\left(\frac{c_1t'}{r}\right)^2-1\right\}^{5/2}}\left(\frac{3D_1}{r}\right)-\frac{1}{\left\{\left(\frac{c_1t'}{r}\right)^2-1\right\}^{3/2}}\left(\frac{D_2}{r}\right)\right.\right.$$

$$\left.-\frac{2\left(\frac{c_1t'}{r}\right)^2-1}{\sqrt{\left(\frac{c_1t'}{r}\right)^2-1}}\left(\frac{2D_3}{r}\right)\right]+\frac{1}{c_2}H\left(\frac{c_2t'}{r}-1\right)\left[\frac{1}{\left\{\left(\frac{c_2t'}{r}\right)^2-1\right\}^{5/2}}\left(\frac{3D_4}{r}\right)\right.$$

$$\left.\left.-\frac{1}{\left\{\left(\frac{c_2t'}{r}\right)^2-1\right\}^{3/2}}\left(\frac{D_5}{r}\right)-\frac{2\left(\frac{c_2t'}{r}\right)^2-1}{\sqrt{\left(\frac{c_2t'}{r}\right)^2-1}}\left(\frac{2D_3}{r}\right)\right]\right\},$$

where $t'=t-\tau$ is the retarded time; $r^2=(x_j-\xi_j)(x_j-\xi_j)$. c_1 and c_2 are propagational velocities of the pressure and shear waves respectively.

In the above expressions, C_1, C_2, C_3 and D_1, D_2, D_3, D_4, D_5 contain spatial terms only and these are presented in Appendix B. These are the non-convoluted form of the volume kernels for dynamic plasticity.

CONSTITUTIVE MODEL

A suitable constitutive model needs to be chosen for dynamic plasticity. The choice of the model should be based on the type of problem, the material properties and the loading conditions. An appropriate material model should also demonstrate a time-dependent viscous behavior. There are a number of various material models available. However, von Mises' constitutive model is used here to study the characteristics of this type of material under dynamic load. Other non-linear material models can be easily incorporated into this algorithm.

The von Mises model describing the incremental stress–strain relation can be expressed as:

$$\Delta\sigma_{ij} = 2\mu\left[\Delta\varepsilon_{ij} + \frac{\nu}{1-\nu}\delta_{ij}\Delta\varepsilon_{kk} - \frac{3S_{ij}S_{kl}}{2\sigma_0^2(1+H/3\mu)}\Delta\varepsilon_{kl}\right], \tag{4}$$

where

$\Delta\sigma_{ij} = D^{ep}_{ijkl}\Delta\varepsilon_{kl}$
$=$ incremental stress tensor,
$\sigma_0 =$ uniaxial yield stress $= \sqrt{\frac{3}{2}S_{ij}S_{ij}}$,
$S_{ij} =$ deviatoric stress tensor $= \sigma_{ij} - \delta_{ij}\sigma_{kk}/3$,
$H =$ slope of the uniaxial plastic stress–strain curve.

NUMERICAL IMPLEMENTATION

Equations (1), (2), (3) and (4) can be regarded as the coupled system of equations for dynamic plasticity. The numerical implementation of eqns (1) and (2) involve volume integration in addition to surface integration. The discretization of the volume is limited to the region where non-linearity is expected. Before describing the spatial discretization, the temporal discretization will be stated first.

(i) *Temporal discretization*

The time axis t is discretized into N equal time steps of duration Δt such that $t = N\Delta t$. The field variables are assumed to vary linearly during a time step and are expressed as:

$$f_i(x,\tau) = M_1(\tau)f_i^n(x) + M_2(\tau)f_i^{n-1}(x),$$

where $f_i(x,\tau)$ stands for displacement, traction or initial stresses. $M_1(\tau)$ and $M_2(\tau)$ are linear temporal shape functions, given by: $M_1(\tau) = (\tau - t_{n-1})/\Delta t$, $M_2(\tau) = (t_n - \tau)/\Delta t$; $t_{n-1} < \tau < t_n$, where the subscripts 1 and 2 refer to the forward and backward temporal nodes, respectively, during a time step.

The terms involving time are simple enough to carry out the temporal integration analytically. After temporal integration, one obtains, from eqns (1) and (2):

$$c_{ij}(\xi)\Delta u_i^N(\xi) = \sum_{n=1}^{N}\left[\int_S [\{G_{ij_1}^{N-n+1} + G_{ij_2}^{N-n}\}\Delta t_i^n - \{F_{ij_1}^{N-n+1} + F_{ij_2}^{N-n}\}\Delta u_i^n\right] dS + \int_V \{B_{ikj}^{N-n+1} + B_{ikj}^{N-n}\}\Delta\sigma_{ik}^{0n}\, dV, \quad (5)$$

and

$$\Delta\sigma_{ij}^N(\xi) = \sum_{n=1}^{N}\left[\int_S [\{G_{kij_1}^{\sigma^N\ N-n+1} + G_{kij_2}^{\sigma^N\ N-n}\}\Delta t_i^n - \{F_{kij_1}^{\sigma^N\ N-n+1} + F_{kij_2}^{\sigma^N\ N-n}\}\Delta u_i^n\right] dS + \int_V \{P_{klij_1}^{N-n+1} + P_{klij_2}^{N-n}\}\Delta\sigma_{ik}^{0n}\, dV + J_{klij}\Delta\sigma_{kl}^{0N}. \quad (6)$$

Terms appearing within the braces are presented in the Appendices.

Note that eqn (3) for the surface stresses does not require any convolution.

(ii) *Spatial discretization*

The boundary discretization is carried out using isoparametric quadratic elements. The coordinates and the functions (incremental displacements and tractions) at any point over a boundary element can be expressed in terms of the nodal values as:

$$x_i = N_\alpha(\eta)X_{i\alpha}, \quad \Delta u_i = N_\alpha(\eta)\Delta U_{i\alpha}, \quad \Delta t_i = N_\alpha(\eta)\Delta T_{i\alpha},$$

where

$$i = 1, 2 \quad \text{and} \quad \alpha = 1, 2, 3.$$

$N_\alpha(\eta)$ are the shape functions in the intrinsic coordinates (η) of the element.

Since the inelastic stresses vanish except in regions of non-linear material response, the volume discretization is required only where non-linearity is expected. The volume is discretized with six- or eight-noded quadratic two-dimensional cells (Fig. 1). The geometry and initial stresses with a cell are given by,

$$x_i = M_\alpha(\eta)X_{i\alpha}, \quad \Delta\sigma_{ij}^0 = M_\alpha(\eta)\Delta\sigma_{ij\alpha}^0,$$

where

x_i = Cartesian coordinates of the cell,
$X_{i\alpha}$ = nodal coordinates of the cell,
η = intrinsic coordinates,
α = number of nodes in the cell (six or eight),
$\Delta\sigma_{ij\alpha}^0$ = nodal value of the incremental stress,
$M_\alpha(\eta)$ = isoparametric shape functions for the volume cell.

With this spatial discretization, eqn (5) takes the form:

$$c_{ij}(\xi)\Delta u_i^N(\xi) = \sum_{n=1}^{N}\left\{\sum_{m=1}^{M}\left[\Delta T_{i\alpha}^n \int_{S_m} \{G_{ij_1}^{N-n+1} + G_{ij_2}^{N-n}\}N_\alpha\, dS - \Delta U_{i\alpha}^n \int_{S_m} \{F_{ij_1}^{N-n+1} + F_{ij_2}^{N-n}\}N_\alpha\, dS\right] + \sum_{m=1}^{L}\left[\Delta\sigma_{ik\alpha}^{0m} \int_{V_m} \{B_{ikl_1}^{N-n+1} + B_{ikl_2}^{N-n}\}M_\alpha\, dV\right]\right\}, \quad (7)$$

where

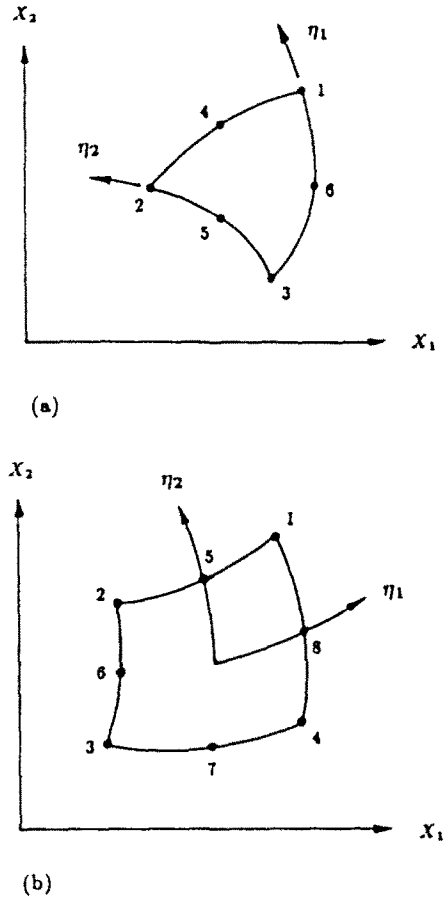

Fig. 1. Two-dimensional volume cells: (a) Six-noded triangle. (b) Eight-noded quadrilateral.

S_m = mth boundary element,
V_m = mth volume cell,
M = total number of boundary elements,
L = total number of volume cells.

Similarly, eqn (6) takes the following form:

$$\Delta\sigma_{ij}^{N}(\xi) = \sum_{n=1}^{N}\left\{\sum_{m=1}^{M}\left[\Delta T_{i\alpha}^{n}\int_{S_m}\{G_{kij_1}^{\sigma^N\,N-n+1}+G_{kij_2}^{\sigma^N\,N-n}\}N_\alpha\,\mathrm{d}S-\Delta U_{i\alpha}^{n}\int_{S_m}\{F_{kij_1}^{\sigma^N\,N-n+1}+F_{kij_2}^{\sigma^N\,N-n}\}N_\alpha\,\mathrm{d}S\right]\right.$$
$$\left.+\sum_{m=1}^{L}\left[\Delta\sigma_{kl\alpha}^{nm}\int_{V_m}\{P_{klij_1}^{N-n+1}+P_{klij_2}^{N-n}\}M_\alpha\,\mathrm{d}V\right]+J_{klij}\Delta_{kl}^{nm}\right\}. \quad (8)$$

The transient kernels appearing in eqns (7) and (8) have sharp variations over space. Hence, the numerical integration (using Gaussian quadrature) of these terms needs intelligent element/cell subdivision with optimum Gauss points in each sub-segment. Moreover, depending on whether the source point (ξ) lies on the element or cell being integrated, the spatial integral can be categorized into the following three types:

(i) ξ does not lie on the element or cell being integrated;
(ii) ξ lies on the element or cell being integrated but the integral is weakly singular;
(iii) ξ lies on the element or cell being integrated but the integral is strongly singular.

The first type of integrals involve the bulk of the computational effort. These integrations are carried out by subdividing each element or cell into a number of sub-elements or sub-cells. For surface elements, this technique has been described in Lachat and Watson (1976) for elasto-static problems while Banerjee and Raveendra (1986) have discussed the integration of volume cells in the context of static plasticity. In transient dynamic problems, as explained earlier, more element or cell subdivisions are required for accurate evaluation of the integrals. The singular integration of the G_{ij}-kernel over the boundary elements and that of the B_{kij}-kernel over the volume cells belong to the second category of integrals. Their evaluation involves more element cell subsegmentation with suitable mapping to make the kernel-shape function-Jacobian product well behaved over each sub-segment (Banerjee and Raveendra, 1986). The third type of integral involves the singular integration of F_{ij}-kernel and P_{kij}-kernel over the boundary and volume respectively. These are evaluated indirectly as elaborated in the following section.

F_{ij}-kernel. The singular integral involving the F_{ij}^{trans}-kernel has the same type and order of singularity as the corresponding elasto-static kernel during the first time step. This integral is evaluated by adding the singular integral of the elasto-static F_{ij}-kernel and the non-singular integral involving the difference between the transient and elasto-static F_{ij}-kernel. The singular integral of the static F_{ij}-kernel is determined indirectly by using the so-called *rigid body technique*. For a detailed discussion, interested readers are referred to the papers by Ahmad and Banerjee (1988) and Israil and Banerjee (1990b).

It is to be mentioned here that for the above technique to be used, the body must have a closed boundary. Thus for half-plane problems, the region of interest must be enclosed with fictitious boundary elements known as "enclosing elements".

P_{kij}-kernel. The plasticity kernel P_{kij} appearing in eqn (2) is strongly singular when the field point lies in the volume cell being integrated. The results of this integration contribute to the diagonal block of the volume matrix. This integral also has the same type and order of singularity as the corresponding static plasticity kernel. Thus it is evaluated in a procedure similar to that explained in the previous section, i.e. by addition of the singular integral of static P_{kij}-kernel and the non-singular integral involving the difference between the transient and static P_{kij}-kernels. The evaluation of the non-singular integral does not pose any difficulty.

The evaluation of the singular integral involving the static P_{kij}-kernel can be performed by either using analytical jump terms or by using a special technique known as *initial stress expansion technique*. For accuracy, the latter approach is utilized here.

In this procedure, the coefficients of the stress equations related to the non-singular nodes are integrated in the usual manner using Gaussian integration with appropriate cell subdivisions. At the singular node, there are three undetermined coefficients corresponding to the initial stress. These cannot be evaluated easily. In an approach similar to that of *rigid body technique* used in evaluating the diagonal terms for surface equations, each of these coefficients is calculated by assuming an admissible initial stress state and a compatible displacement field. Details of this process can be found in Banerjee *et al.* (1989) and Banerjee and Henry (1989). It is to be mentioned here that for this method, the entire body must be discretized with cells. However, for cases where only a small region of the body is expected to be plastic, it is modeled as a multiply-connected region with full volume discretization used only in the non-linear region, the remaining region(s) having no cell.

SOLUTION PROCEDURE

With the temporal and spatial integration complete, a system of algebraic equations can be developed. This is obtained by sequentially writing eqn (7) for each of the collocation points. The assembled system of equation takes the following matrix form:

$$\sum_{n=1}^{N} [[G_1^{N-n+1} + G_2^{N-n}]\{\Delta T^n\} - [F_1^{N-n+1} + F_2^{N-n}]\{\Delta U^n\} + [B_1^{N-n+1} + B_2^{N-n}]\{\Delta\sigma'^n\}] = \{0\}. \tag{9}$$

At time t, there are as many unknowns as the number of equations. Also the past history (up to time $N-1$) is known. Thus, eqn (9) can be rearranged to:

$$[A^N]\{\Delta X^N\} = [B^n]\{\Delta Y^N\} + [C^n]\{\Delta\sigma'^N\} + \{R^N\}, \tag{10}$$

where $\{\Delta X^N\}$ and $\{\Delta Y^N\}$ are the vectors of the unknown and known incremental boundary quantities and $\{R^N\}$ is the effect of the past dynamic history on the current time node and given by,

$$\{R^N\} = -\sum_{n=1}^{N-1} ([G_1^{N-n+1} + G_2^{N-n}]\{\Delta T^n\} - [F_1^{N-n+1} + F_2^{N-n}]\{\Delta U^n\} + [B_1^{N-n+1} + B_2^{N-n}]\{\Delta\sigma'^n\}).$$

Similarly, the integral equation for stresses, i.e. eqn (8) can be written as,

$$\{\Delta\sigma^N\} = -[A^n]\{\Delta X^N\} + [B^n]\{\Delta Y^N\} + [C^n]\{\Delta'^N\} + \{R^{\sigma N}\}, \tag{11}$$

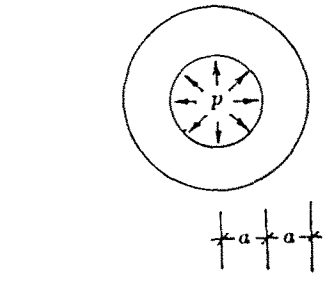

(a)

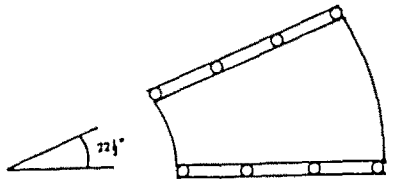

(b)

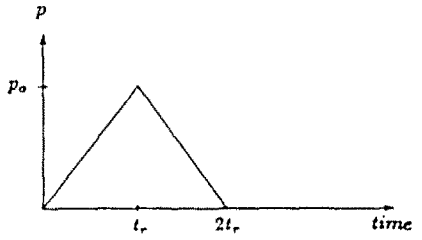

(c)

Fig. 2. (a) Cylinder under transient internal pressure. (b) A $22\frac{1}{2}$ segment of the cylinder (1/8th) used in modeling. (c) Time history of the applied internal pressure.

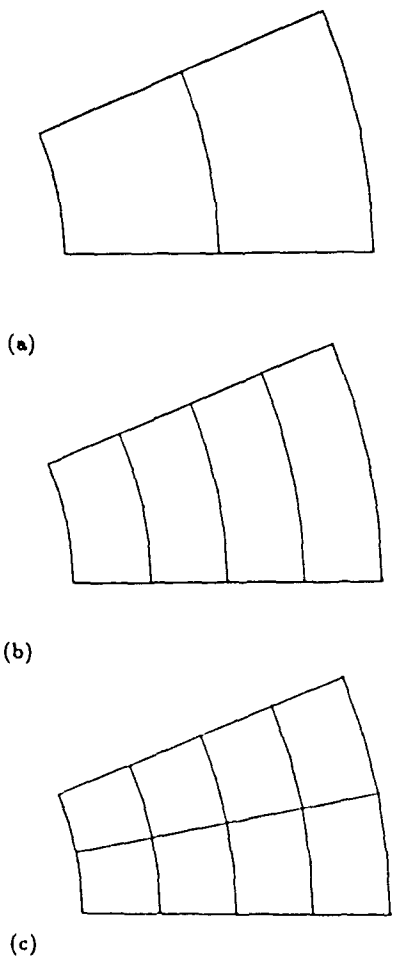

Fig. 3. Three different mesh patterns: (a) Mesh 1 (6 elements; 2 cells). (b) Mesh 2 (10 elements; 4 cells). (c) Mesh 3 (12 elements; 8 cells).

where $[C^a]$ contains the contribution from the jump term J_{klij} in addition to the volume integral of P_{klij}-kernel, and

$$\{R^{a^N}\} = -\sum_{n=1}^{N-1} ([G_1^{a^N\ n+1} + G_2^{a^N\ n}]\{\Delta T^n\} - [F_1^{a^N\ n+1} + F_2^{a^N\ n}]\{\Delta U^n\} + [P_1^{N-n+1} + P_2^{N-n}]\{\Delta\sigma^{in}\}).$$

The system of equations given by eqns (10) and (11) along with the constitutive

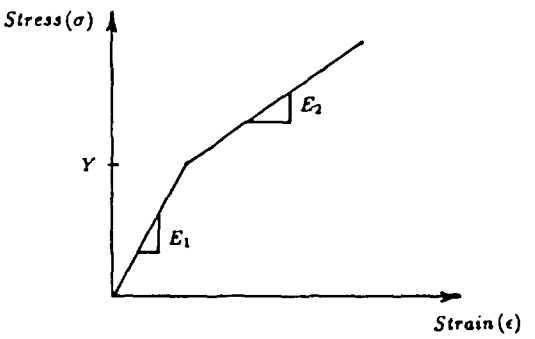

Fig. 4. Stress–strain behavior of the cylinder material.

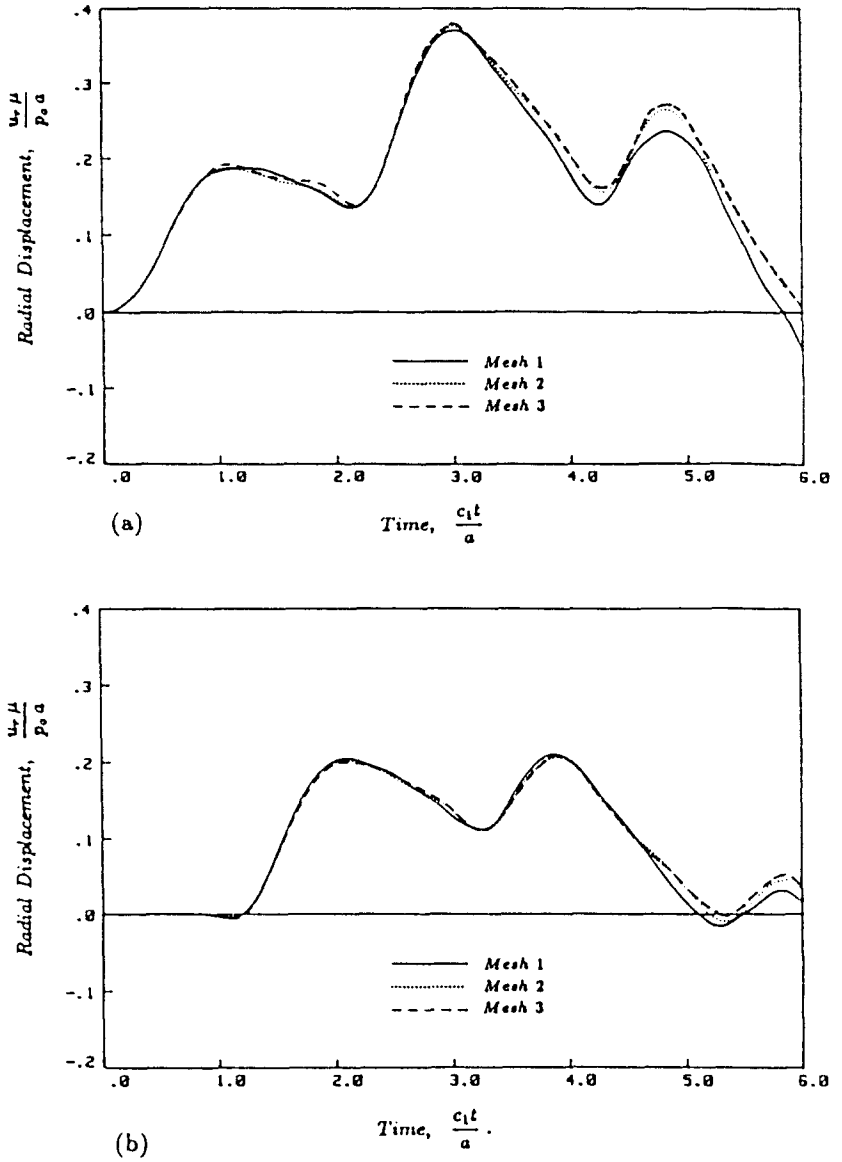

Fig. 5. Time history of the radial displacement of the cylinder using three different mesh: (a) inner surface; (b) outer surface.

equation (4) form the basis of the dynamic plasticity algorithm. However, the solution of eqns (10) and (11) requires the knowledge of initial stresses which are not known *a priori*. Thus an iterative scheme must be used for this process. Ahmad and Banerjee (1990), for their dynamic plasticity algorithm, used the iterative algorithm suggested by Banerjee and Raveendra (1986). However, it was found that for dynamic problems faster and better convergence is achieved by using the so-called "Newton–Raphson" iterative scheme as developed by Chopra and Dargush (1991).

APPLICATIONS

The dynamic plasticity algorithm developed in this chapter is the first of its kind for two-dimensional problems. Thus, it has been very difficult to find any analytical or numerical solution to compare the results from the present methodology. Hence, the accuracy and stability of this method has been established via convergence studies. The first example has been chosen for that purpose. The other example is presented to demonstrate the applicability of this method to practical problems.

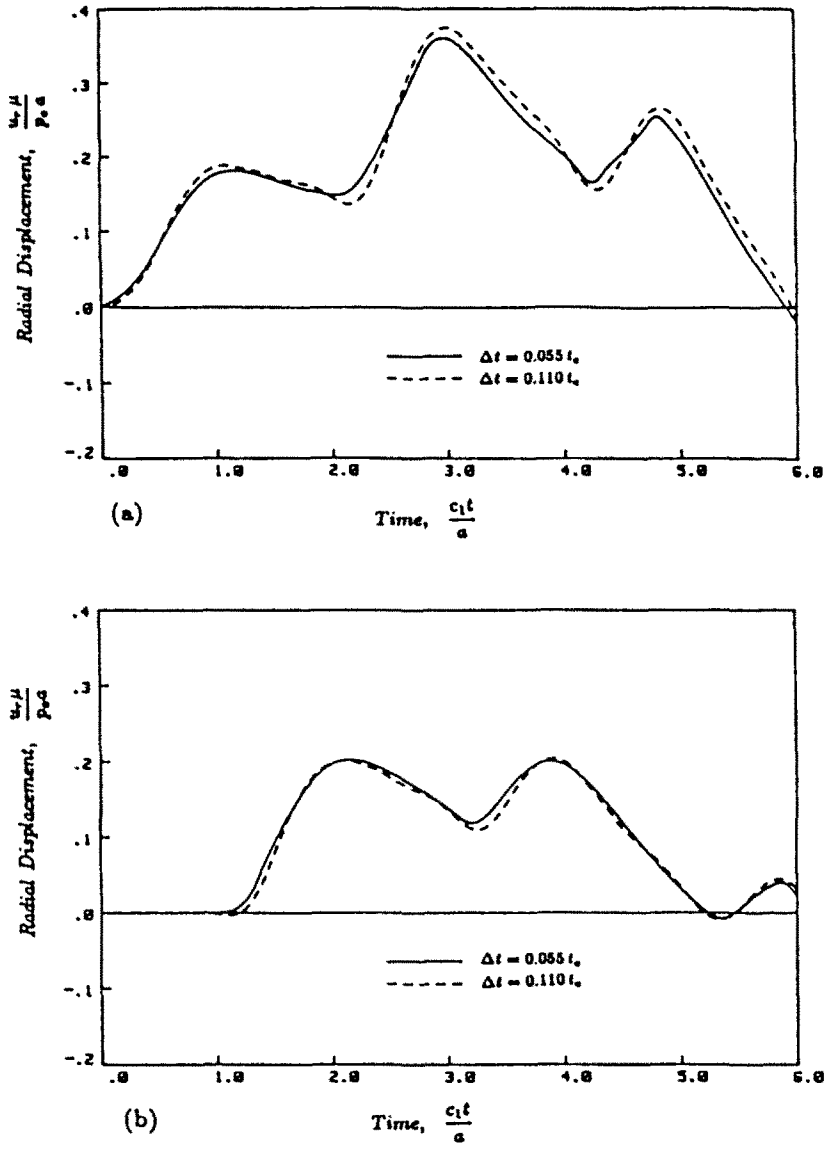

Fig. 6. Time history of the radial displacement of the cylinder using two different time steps (mesh 2): (a) inner surface; (b) outer surface.

Example 1 : *Cylinder under radial pressure*

The cylinder shown in Fig. 2a is subjected to an internal radial pressure the time-history of which is triangular (Fig. 2c). Because of symmetry, only 1/8th of the cylinder needs to be modeled with a roller on the lateral faces (Fig. 2b).

The various geometrical and material properties are presented below:

$$\textit{internal radius}, R_i = a,$$

$$\textit{external radius}, R_e = 2a,$$

$$a = 10; \quad \nu = 0.25; \quad \rho = 1.0,$$

$$\textit{rise time}, t_r = 5\,\text{s}.$$

Convergence studies were carried out with respect to mesh refinement and time-step size. Three different mesh patterns and two different time steps were used. Mesh 1 has two

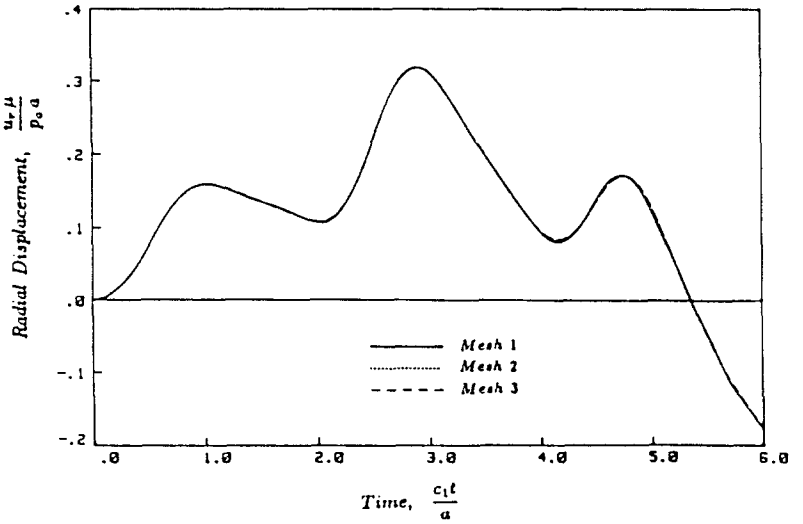

Fig. 7. Time history of the radial displacement of the inner surface of the cylinder using three different mesh (elastic).

volume cells, mesh 2 has four volume cells while mesh 3 contains eight cells. All three meshes are depicted in Fig. 3.

The problem was analyzed assuming it to be both an elastic and an elasto-plastic solid. The stress–strain behavior for the elasto-plastic material is shown in Fig. 4. Also for the non-linear analysis, von Mises' plasticity model was used and the hardening was assumed to be such that $E_2/E_1 = 0.5$. The maximum load intensity was taken as twice the yield capacity, i.e. $p_0 = 2Y$.

The time-history of the radial displacements of the inner and outer surface of the cylinder are plotted in Fig. 5 for the three different mesh patterns. The time step is chosen to be $\Delta t = 0.11 t_c$, where t_c is the time needed by the pressure wave to travel from the inner surface to the outer surface of the cylinder and is given by, $t_c = a/c_1$. The results obtained by the three different meshes agree fairly well with mesh 2 and mesh 3 producing almost identical solutions hence establishing the convergence of the solutions. Mesh 2 was chosen for further study.

Next, analyses were carried out to establish the accuracy with respect to the time steps. Two different time steps were chosen *viz*, $\Delta t = 0.055 t_c$ and $\Delta t = 0.11 t_c$. Results of the analyses are presented in Fig. 6 and the two sets of results agree reasonably well.

Also, similar convergence studies were performed for the elastic analysis with respect to mesh refinements. The radial displacement at the inner surface of the cylinder obtained from the above study is shown in Fig. 7. Identical solutions are obtained from all three meshes establishing the confidence in the results.

Finally, the results from the elastic and elasto-plastic analyses are compared in Fig. 8. The solutions obtained from the elasto-plastic analysis are higher than the elastic analysis, as one would expect.

Example 2: Explosion in an underground cylindrical cavity

An underground cylindrical cavity (Fig. 9) is subjected to a blast load. The time history of the load is triangular (same as in Fig. 2c). The symmetry of the problem dictates that only one-half of the problem is needed to be modeled as shown in Fig. 10. The medium is modeled as a two-region problem. One region (Region I, Fig. 10) is discretized with 34 volume cells where non-linear material behavior is expected. The discretization pattern is depicted in Fig. 11. The other region (Region II, Fig. 10) where only linear behavior is expected has only boundary discretization. The semi-infinite part is modeled with "enclosing elements" for proper evaluation of the jump terms. The various problem parameters are:

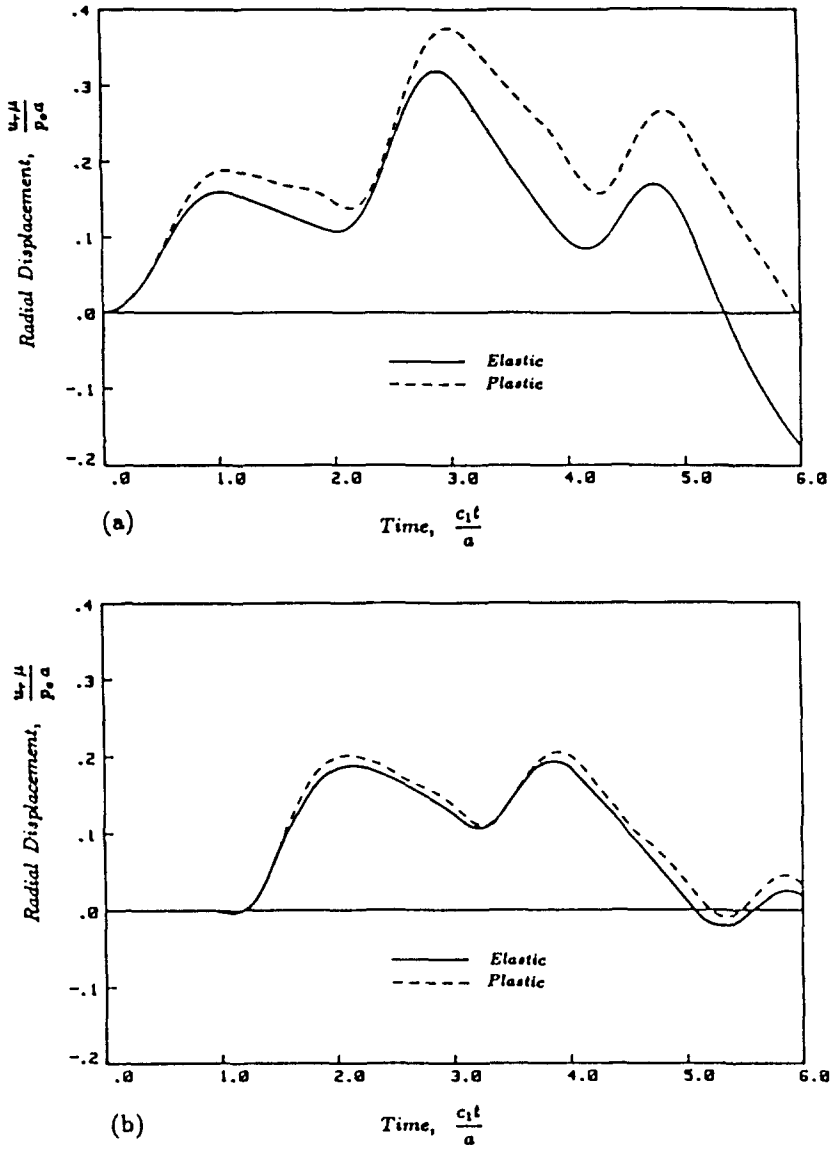

Fig. 8. Comparison of the radial displacement of the cylinder obtained via elastic and elasto-plastic analysis: (a) inner surface; (b) outer surface.

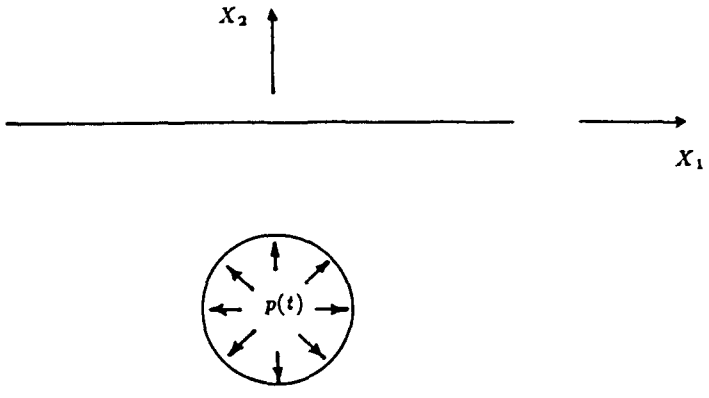

Fig. 9. Explosion in an underground cylindrical cavity.

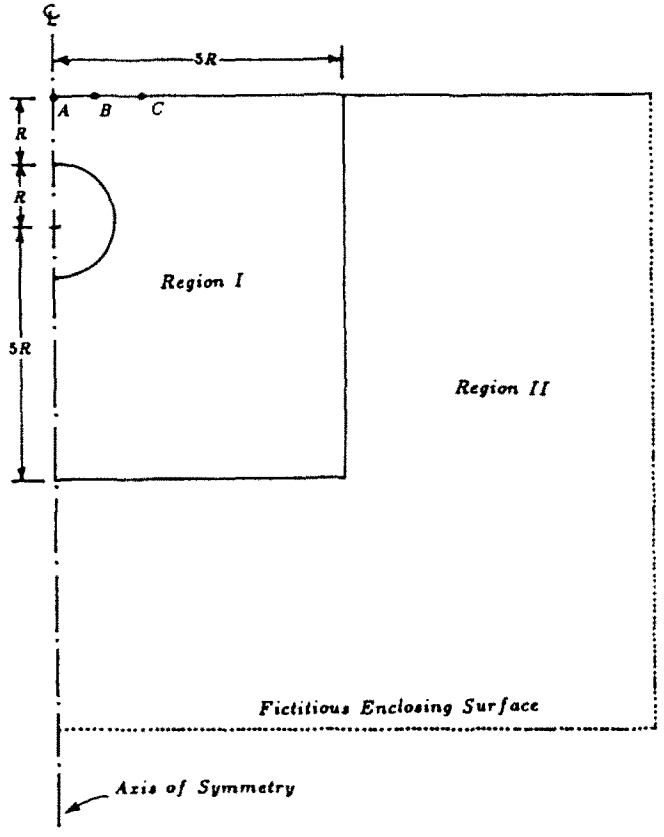

Fig. 10. The problem modeled as two regions: Region I: volume discretization. Region II: no volume discretization.

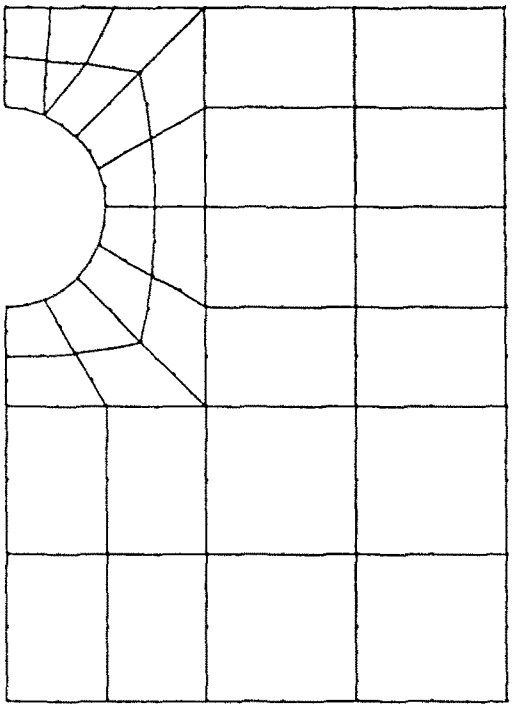

Fig. 11. Region I: discretized with 34 volume cells.

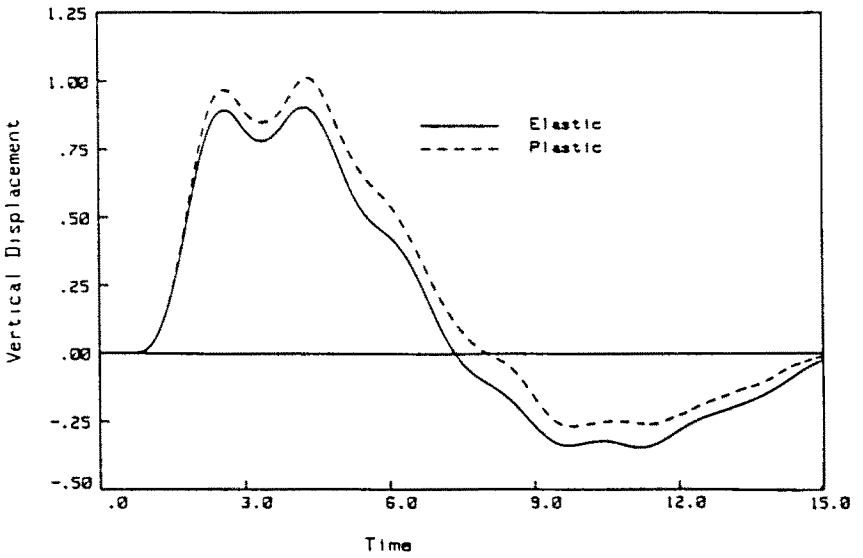

Fig. 12. Time history of vertical displacement of A (0, 0).

$$R = 1, \quad \rho = 1, \quad t_r = 1 \text{ s}.$$

For the non-linear analysis, the maximum load intensity (p_0) is taken as twice the yield strength. The hardening is chosen such that $E_2/E_1 = 0.8$ (Fig. 4). In this example also, von Mises' plasticity model and normalized displacements (UE/p_0R) are plotted against non-dimensional time (C_1t/R) is used.

The displacements at a few selected surface points are investigated. The time history of vertical displacements at points $A(0, 0)$, $B(0.45R, 0)$ and $C(1.1R, 0)$ are presented in Figs 12, 13 and 14, respectively. The displacements obtained from the non-linear analysis are higher than the elastic case, as expected. The history of horizontal displacements at points B and C are depicted in Figs 15 and 16. The non-linear behavior is similar to the vertical

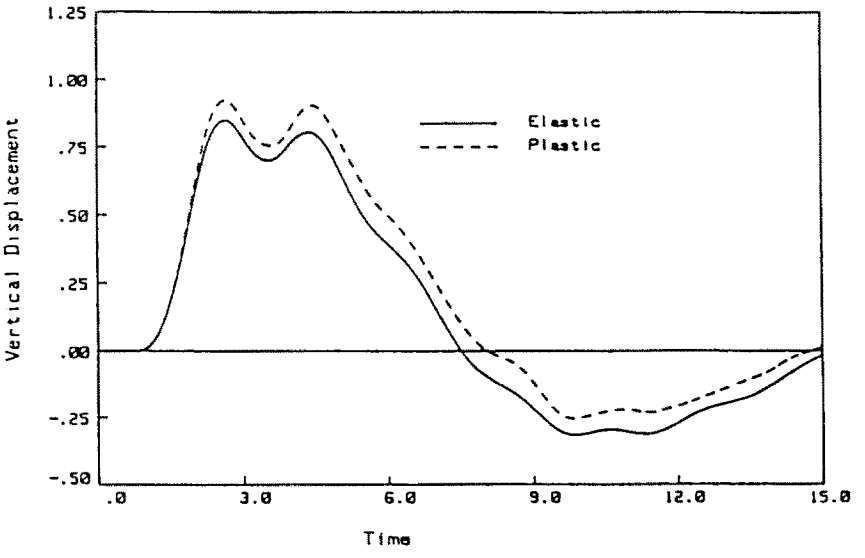

Fig. 13. Time history of vertical displacement at B (0.45R, 0).

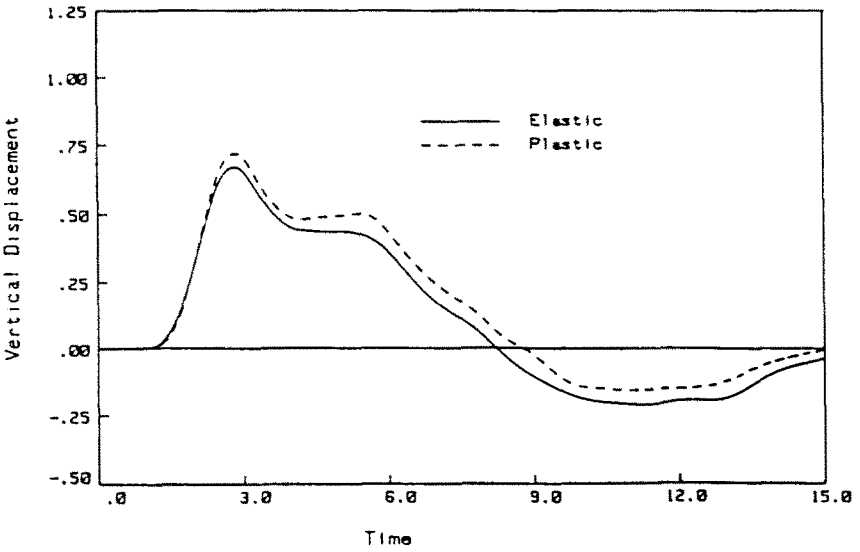

Fig. 14. Time history of vertical displacement at C $(1.1R, 0)$.

case. However, the horizontal displacement at location C is found to be higher than at location B.

CONCLUSION

An advanced development of the time-domain boundary element method for two-dimensional problems of dynamic elasto-plasticity is presented. This algorithm incorporates higher order spatial and temporal variations of the field quantities. Von Mises' material model is used for simplicity, although any other material model can be easily incorporated in the formulation. The formulation is found to produce static plasticity results when the time step is very large. When the yield stress was selected to be very large compared to the applied stress, the results were the same as those obtained from a linear elastodynamic analysis. Both of these help establish the validity of the algorithm. Because of the unavailability of any published results in this area, no comparative study could be provided. Hence, the accuracy of the methodology is established via convergence studies.

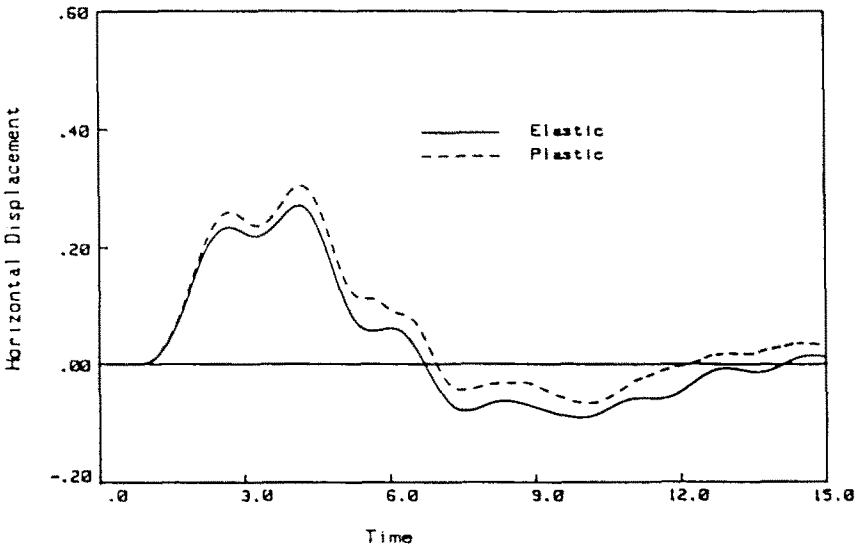

Fig. 15. Time history of horizontal displacement at B.

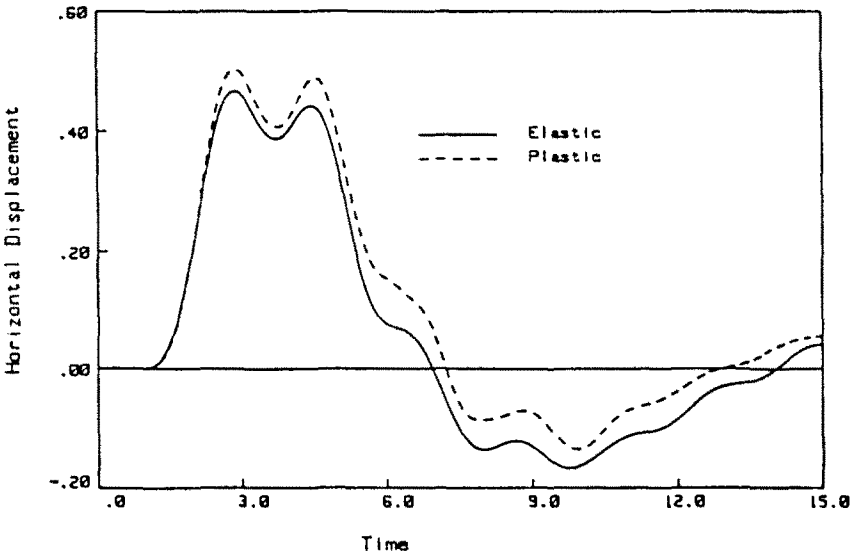

Fig. 16. Time history of horizontal displacement at C.

REFERENCES

Ahmad, S. and Banerjee, P. K. (1990). Inelastic transient dynamic analysis of three-dimensional problems by BEM. *Int. J. Num. Meth. Engng* **29**, 371–390.

Banerjee, P. K. and Butterfield, R. (1981). *Boundary Element Method in Engineering Science*. McGraw-Hill, London and New York.

Banerjee, P. K., Cathie, D. N. and Davies, T. G. (1979). Two- and three-dimensional problems of elastoplasticity. In *Developments in Boundary Elements* (Edited by P. K. Banerjee and R. Butterfield), Vol. 1. Applied Science Publishers, London.

Banerjee, P. K. and Henry, D. P. (1989). Advanced applications of BEM to inelastic analysis of solids. In *Developments in Boundary Element Methods* (Edited by P. K. Banerjee and R. B. Wilson), Vol. 5. Elsevier Applied Science, London and New York.

Banerjee, P. K., Henry, D. P. and Raveendra, S. T. (1989). Advanced inelastic analysis of solids by the boundary element method. *Int. J. Mech. Sci.* **31**, 309–322.

Banerjee, P. K. and Raveendra, S. T. (1986). Advanced boundary element analysis of two- and three-dimensional problems of elastoplasticity. *Int. J. Num. Meth. Engng* **23**, 985–1002.

Cathie, D. N. and Banerjee, P. K. (1980). Boundary element methods for axisymmetric plasticity. In *Innovative Numerical Methods for the Applied Engineering Science* (Edited by R. P. Shaw, W. Pilkey, R. Wilson, Al. Lakis, A. Choudonet and C. Morino), pp. 331–339. University of Virginia Press, VA.

Chopra, M. and Dargush, G. F. (1991). An advanced boundary element method for elasto-plasticity. (In preparation.)

Israil, A. S. M. and Banerjee, P. K. (1990a). Advanced time-domain formulation of BEM for two-dimensional transient elastodynamics. *Int. J. Num. Meth. Engng* **29**, 1421–1440.

Israil, A. S. M. and Banerjee, P. K. (1990b). Two-dimensional transient wave-propagation problems by time-domain BEM. *Int. J. Solids Structures* **26**, 851–864.

Israil, A. S. M. and Banerjee, P. K. (1991). Interior stress calculations in 2-D time-domain transient BEM analysis. *Int. J. Solids Structures* **27**(7), 915–927.

Lachat, J. C. and Watson, J. O. (1976). Effective numerical treatment of boundary integral equations: a formulation for three-dimensional elasto-statics. *Int. J. Num. Meth. Engng* **10**, 991–1005.

Mansur, W. J. (1983). A time-stepping technique to solve wave propagation problems using the boundary element method. Ph.D. Dissertation, Southampton University.

Mukherjee, S. (1982). *Boundary Elements in Creep and Fracture*. Elsevier Applied Sciences Publishers, London.

Riccardella, P. (1973). An implementation of boundary integral technique for planar problems of elasticity and elastoplasticity. Ph.D. Dissertation, Carnegie-Mellon University.

APPENDIX A

Boundary kernels

$$G_{ij_1}^{N-n+1}+G_{ij_2}^{N-n}=\frac{1}{2\pi\rho}\sum_{\alpha=1}^{2}\frac{1}{c_\alpha^2}\left[\frac{\delta_{ij}}{2}\left[N\cosh^{-1}\left(\frac{c_\alpha N\Delta T}{r}\right)-2(N-1)\cosh^{-1}\left\{\frac{c_\alpha(N-1)\Delta T}{r}\right\}\right.\right.$$
$$\left.+(N-2)\cosh^{-1}\left\{\frac{c_\alpha(N-2)\Delta T}{r}\right\}\right]+(-1)^n\{(\delta_{ij}-2r_{,i}r_{,j})\left(\frac{c_\alpha\Delta T}{r}\right)^2 S_\alpha-(-1)^n\{(\delta_{ij}-2r_{,i}r_{,j})Q_\alpha$$
$$\left.-(-1)^n(\delta_{ij}\delta_{2\alpha}-r_{,i}r_{,j})P_\alpha\right] \quad \text{(A1)}$$

$$F_{ij_1}^{N-n+1}+F_{ij_2}^{N-n}=\frac{\mu}{2\pi\rho r}\sum_{\alpha=1}^{2}\left[\left\{\frac{-A_1\delta_{1\alpha}+A_3\delta_{2\alpha}}{c_\alpha^2}\right\}P_\alpha-(-1)^\alpha A_2\left(\frac{\Delta T}{r}\right)^2 Q_\alpha\right]. \tag{A2}$$

where

$$S_\alpha=(N-n+1)^2\sqrt{(N-n+1)^2-\left(\frac{r}{c_\alpha\Delta T}\right)^2}-2(N-n)^2\sqrt{(N-n)^2-\left(\frac{r}{c_\alpha\Delta T}\right)^2}$$
$$+(N-n-1)^2\sqrt{(N-n-1)^2-\left(\frac{r}{c_\alpha\Delta T}\right)^2}$$

$$P_\alpha=\sqrt{(N-n+1)^2-\left(\frac{r}{c_\alpha\Delta T}\right)^2}-2\sqrt{(N-n)^2-\left(\frac{r}{c_\alpha\Delta T}\right)^2}+\sqrt{(N-n-1)^2-\left(\frac{r}{c_\alpha\Delta T}\right)^2}$$

$$Q_\alpha=\left\{(N-n+1)^2-\left(\frac{r}{c_\alpha\Delta T}\right)^2\right\}^{1/2}-2\left\{(N-n)^2-\left(\frac{r}{c_\alpha\Delta T}\right)^2\right\}^{1/2}+\left\{(N-n-1)^2-\left(\frac{r}{c_\alpha\Delta T}\right)^2\right\}^{1/2}$$

with $\alpha=1, 2$.

$$A_1=\frac{\lambda}{\mu}n_i r_{,j}+2r_{,i}r_{,j}\frac{\partial r}{\partial n},\quad A_2=n_i r_{,j}+n_j r_{,i}+\frac{\partial r}{\partial n}(\delta_{ij}-4r_{,i}r_{,j}),\quad A_3=\frac{\partial r}{\partial n}(2r_{,i}r_{,j}-\delta_{ij})-n_j r_{,i}.$$

APPENDIX B

Interior stress kernels

$$G_{kij_1}^{N-n+1}+G_{kij_2}^{N-n}=\frac{\mu}{2\pi\rho r}\left[\frac{B_1}{c_1^2}P_1-\frac{B_3}{c_2^2}P_2+\tfrac{1}{2}B_2\left(\frac{\Delta T}{r}\right)^2(Q_2-Q_1)\right] \tag{B1}$$

$$F_{kij_1}^{N-n+1}+F_{kij_2}^{N-n}=\frac{\mu^2}{2\pi\rho r^2}\left[\frac{-2(E_1+E_2)}{c_1^2}P_1+\frac{2(E_4+E_5)}{c_2^2}P_2+\tfrac{1}{2}E_3\left(\frac{\Delta T}{r}\right)^2(Q_1-Q_2)-\frac{E_1}{c_1^2}R_1+\frac{E_4}{c_2^2}R_2\right], \tag{B2}$$

where, P_α and Q_α have been defined in the previous section.

$$R_\alpha=\left(\frac{r}{c_\alpha\Delta T}\right)^2\left[\frac{1}{\sqrt{(N-n+1)^2-\left(\frac{r}{c_\alpha\Delta T}\right)^2}}-2\frac{1}{\sqrt{(N-n)^2-\left(\frac{r}{c_\alpha\Delta T}\right)^2}}+\frac{1}{\sqrt{(N-n-1)^2-\left(\frac{r}{c_\alpha\Delta T}\right)^2}}\right],$$

with $\alpha=1, 2$.

$$B_1=\frac{\lambda}{\mu}\delta_{ij}r_{,k}+2r_{,i}r_{,j}r_{,k},\quad B_2=r_{,i}\delta_{jk}+r_{,j}\delta_{ik}+r_{,k}\delta_{ij}-4r_{,i}r_{,j}r_{,k},\quad B_3=2r_{,i}r_{,j}r_{,k}-r_{,i}\delta_{jk}-r_{,j}\delta_{ik},$$

$$E_1=\left(\frac{\lambda}{\mu}\delta_{ij}+2r_{,i}r_{,j}\right)\left(\frac{\lambda}{\mu}n_k+2\frac{\partial r}{\partial n}r_{,k}\right),$$

$$E_2=-n_k\left[\frac{\lambda}{\mu}\delta_{ij}(2+\lambda/\mu)+2r_{,i}r_{,j}\right]-2n_i r_{,j}r_{,k}-2n_j r_{,i}r_{,k}-2\frac{\partial r}{\partial n}(r_{,i}\delta_{jk}+r_{,j}\delta_{ik}+r_{,k}\delta_{ij}-6r_{,i}r_{,j}r_{,k}),$$

$$E_3=n_i(-\delta_{jk}+4r_{,j}r_{,k})+n_j(-\delta_{ik}+4r_{,i}r_{,k})+n_k(-\delta_{ij}+4r_{,i}r_{,j})+4\frac{\partial r}{\partial n}(r_{,i}\delta_{jk}+r_{,j}\delta_{ik}+r_{,k}\delta_{ij}-6r_{,i}r_{,j}r_{,k}),$$

$$E_4=\frac{\partial r}{\partial n}(4r_{,i}r_{,j}r_{,k}-r_{,i}\delta_{jk}-r_{,j}\delta_{ik})-n_i r_{,j}r_{,k}-n_j r_{,i}r_{,k},$$

$$E_5=n_i(\delta_{jk}-2r_{,j}r_{,k})+n_j(\delta_{ik}-2r_{,i}r_{,k})-2n_k r_{,i}r_{,j}-2\frac{\partial r}{\partial n}(r_{,i}\delta_{jk}+r_{,j}\delta_{ik}+r_{,k}\delta_{ij}-6r_{,i}r_{,j}r_{,k}).$$

APPENDIX C

Volume kernels for plasticity

$$B^{\alpha,\,\mathrm{elas}}_{kij} + B^{\alpha,\,\mathrm{p}}_{kij} = \frac{\mu}{2\pi\rho r}\left[\frac{C_1}{c_1^2}P_1 - \frac{C_3}{c_2^2}P_2 + \tfrac{1}{2}C_2\left(\frac{\Delta T}{r}\right)^2(Q_2 - Q_1)\right] \tag{C1}$$

$$P^{\alpha,\,\mathrm{elas}}_{kij} + P^{\alpha,\,\mathrm{p}}_{kij} = \frac{\mu}{2\pi\rho r^3}\left[\frac{-2(D_1+D_2)}{c_1^2}P_1 + \frac{2(D_4+D_5)}{c_2^2}P_2 + \tfrac{1}{2}D_3\left(\frac{\Delta T}{r}\right)^2(Q_1 - Q_2) - \frac{D_1}{c_1^2}R_1 + \frac{D_4}{c_2^2}R_2\right], \tag{C2}$$

where P_α, Q_α and R_α have been defined earlier, with $\alpha = 1, 2$.

$$C_1 = r_{,i}r_{,j}r_{,k}, \quad C_2 = r_{,i}\delta_{jk} + r_{,j}\delta_{ik} + r_{,k}\delta_{ij} - 4r_{,i}r_{,j}r_{,k}, \quad C_3 = r_{,i}r_{,j}r_{,k} - \tfrac{1}{2}r_{,i}\delta_{jk} - \tfrac{1}{2}r_{,j}\delta_{ik},$$

$$D_1 = r_{,k}r_{,l}\left(\frac{\lambda}{\mu}\delta_{ij} + 2r_{,i}r_{,j}\right),$$

$$D_2 = -\frac{\lambda}{\mu}\delta_{ij}\delta_{kl} + 2(-r_{,i}r_{,k}\delta_{jl} - r_{,i}r_{,j}\delta_{kl} - r_{,k}r_{,l}\delta_{ij} - r_{,i}r_{,l}\delta_{kj} - r_{,j}r_{,k}\delta_{il} - r_{,j}r_{,l}\delta_{ik} + 6r_{,i}r_{,j}r_{,k}r_{,l}),$$

$$D_3 = \delta_{ij}(-\delta_{kl} + 4r_{,k}r_{,l}) + \delta_{ik}(-\delta_{jl} + 4r_{,j}r_{,l}) + \delta_{jk}(-\delta_{il} + 4r_{,i}r_{,l}) + 4(r_{,i}r_{,j}\delta_{kl} + r_{,i}r_{,k}\delta_{jl} + r_{,j}r_{,k}\delta_{il} - 6r_{,i}r_{,j}r_{,k}r_{,l}),$$

$$D_4 = 2r_{,i}r_{,j}r_{,k}r_{,l} - \tfrac{1}{2}r_{,i}r_{,j}\delta_{kl} - \tfrac{1}{2}r_{,j}r_{,l}\delta_{ik} - \tfrac{1}{2}r_{,i}r_{,k}\delta_{jl} - \tfrac{1}{2}r_{,j}r_{,k}\delta_{il},$$

$$D_5 = \delta_{ik}\delta_{jl} + \delta_{jk}\delta_{il} + 2(-r_{,i}r_{,k}\delta_{jl} - r_{,i}r_{,j}\delta_{kl} - r_{,k}r_{,l}\delta_{ij} - r_{,j}r_{,k}\delta_{il} - r_{,j}r_{,l}\delta_{ik} + 6r_{,i}r_{,j}r_{,k}r_{,l}).$$